PHOTODISINTEGRATION CROSS SECTION OF BERYLLIUM NEAR THRESHOLD

JOHN M. PROSSER

mo

UCRL-5996

UNIVERSITY OF CALIFORNIA
Lawrence Radiation Laboratory
Livermore, California

PHOTODISINTEGRATION CROSS SECTION OF BERYLLIUM NEAR THRESHOLD

John M. Prosser

12 May 1960

Submitted in partial fulfillment
of the requirements for the degree of

MASTER OF SCIENCE
IN
PHYSICS

United States Naval Postgraduate School
Monterey, California

PHOTODISINTEGRATION CROSS SECTION OF BERYLLIUM NEAR THRESHOLD

John M. Prosser and Walter John, Jr.

Lawrence Radiation Laboratory, University of California
Livermore, California

12 May 1960

ABSTRACT

The cross section for photoneutron production in Be^9 at energies of 1.692, 1.720, and 1.78 Mev has been investigated using radioisotope gamma-ray sources. Neutron counting was by manganous sulfate bath and a long counter. Gamma-ray counting was by a scintillation spectrometer consisting of a NaI(Tl) scintillation crystal and a 256-channel pulse-height analyzer. The following results were obtained:

$$\sigma_{1.692} = 1.35 \pm 0.08 \text{ mb}$$

$$\frac{\sigma_{1.720}}{\sigma_{1.692}} = 0.763 \pm 0.022$$

$$\frac{\sigma_{1.78}}{\sigma_{1.692}} = 0.617 \pm 0.013$$

A theoretical treatment of the $P \rightarrow S$ transition near threshold using square-well potentials is also presented.

I. INTRODUCTION

The photoneutron cross section in beryllium is of great interest for several reasons: (1) beryllium has the lowest threshold for this reaction of any element; (2) beryllium is used in many photoneutron sources where a supply of monoenergetic neutrons is desired; (3) beryllium is often used

as a reflector in nuclear reactors; (4) the photodisintegration cross section may be used as a test for models of the beryllium nucleus. The photoneutron reaction was discovered in 1934 by Chadwick and Goldhaber (Ch34), who observed the reaction in deuterium, and in the same year Szilard and Chalmers (Sz34) observed the reaction in beryllium. Early measurements of the cross section for photoneutron production in beryllium were attempted by several experimenters, with widely varying results. The cross section was calculated theoretically by Guth and Mullin (Gu49) in 1949, and their results have been fairly well accepted until very recently. The most recent theory is essentially similar to that of Guth and Mullin, but substitutes a potential of the Saxon type for the square well originally used, resulting in a considerably better fit with experimentally determined points.

This paper will present a brief discussion of photoneutron reactions in general, some discussion of the theory, a discription of several new experiments measuring the cross section at different energies, and conclusions drawn from these experiments.

II. GENERAL

Neutrons were first discovered in 1930, having been produced by the (α, n) reaction. The (γ, n) reaction was then discovered in 1934, when neutrons were observed to result from the irradiation of beryllium and deuterium by high-energy gamma rays. Further investigation showed that these photoneutrons were emitted with a well-defined energy spectrum, in contrast with those resulting from alpha-particle bombardment, which have a widely distributed energy spectrum. In many applications, this discrete energy characteristic is very useful. Unfortunately, however, there is an attendant disadvantage. The cross section for the production of photoneutrons is very small, so that in order to produce a reasonable neutron flux a gamma-ray source of very high intensity must be employed. Unlike the alpha particles, which are stopped within the source, the gamma-ray intensity is attenuated only negligibly, thus producing high gamma-ray backgrounds and making handling conditions difficult.

(γ, n) reactions in general involve the absorption of a gamma photon into the nucleus, forming an excited nucleus which then decays with the emission of a neutron. Thus

$$E_n = E_\gamma - (\text{binding energy}).$$

From this it becomes apparent that if the gamma-ray energy is well-defined, the neutron energy will also be well-defined. The best source of monoenergetic gamma rays is the radiation from radioisotopes. Unfortunately, the useful gamma rays (that is, those having a long half-life and high yield) are limited to energies of less than 3 Mev. Although the (γ, n) reaction occurs in many elements, only deuterium and beryllium have thresholds below 3 Mev for this reaction. By the use of various radioisotopes these two elements have been employed in sources for the production of monoenergetic neutrons with energies from 25 to 1000 kev. Photoneutrons can also be produced by the use of bremsstrahlung from targets bombarded by high-energy electrons from an accelerator, but these neutrons are not monoenergetic due to the continuous energy spectrum of the bremsstrahlung.

III. THE (γ, n) REACTION IN BERYLLIUM

Photoneutrons are produced from beryllium by the following reaction for gamma-ray energies less than about 2.5 Mev:

$$h\nu + Be^9 \rightarrow Be^8 + n - 1.666 \text{ Mev}$$

In this reaction the Be^8 is left in its ground state and decays with a half-life of $\sim 10^{-15}$ second as follows:

$$Be^8 \rightarrow 2\,He^4 + 0.09 \text{ Mev}$$

It would appear that the reaction

$$h\nu + Be^9 \rightarrow 2\,He^4 + n - 1.576 \text{ Mev}$$

is favored energetically, since it has a lower threshold. In 1952 Alburger (Al52) looked for this reaction, using 1.631-Mev gamma rays from Ne^{20},

and observed no neutrons which could be attributed to this reaction. On the basis of this experiment he concluded that the cross section for the reaction could not be greater than 10^{-30} cm^2.

At gamma-ray energies higher than about 2.5 Mev many other reactions are possible. These have been summarized by Paolini in a recent paper (Pa60) and will not be repeated here.

The total cross section for the $Be^9(\gamma, n)Be^8$ reaction has been measured experimentally at several energies using radioisotope sources. Some of the more important of these are listed in Table I.

TABLE I

Measurements of Photoneutron Cross Sections for Beryllium Near Threshold

Gamma source	Gamma energy (Mev)	Cross section (mb)	Reference
Sb^{124}	1.692	1.0 mb	Note 1
		1.9	Note 2
		1.262 ± 0.069	(Gi59)
		1.35 ± 0.08	This paper
Bi^{206}	1.720	1.03 ± 0.07	This paper
Al^{28}	1.78	0.83 ± 0.06	This paper
Y^{88}	1.85	0.654 ± 0.031	(Gi59)
		0.55	Note 3
Pr^{144}	2.185	0.39	(Ha53)
MsTh	2.61	0.50	(Al50) + (Bi50)
		0.377 ± 0.02	(Ed56)
Na^{24}	2.754	0.70	(Ru48)
		0.674	(Sn50)

Notes:

1. Unpublished. Found by A. H. Snell about 1946.
2. Obtained from (Ru48) by application of branching ratio.
3. Unpublished. Found by E. Segrè in 1949.

In 1956 Connors and Miller (Co56) explored the cross section near threshold using bremsstrahlung from an accelerator and reported a peak at 1.70 ± 0.05 Mev, with the cross section $\geq$ 200 times the average cross section in this energy region, and with a peak width $\leq$ 50 kev. A more recent experiment by Walter, Shea, and Miller (Wa60) fails to show such a peak. In this experiment they also used bremsstrahlung from an electron accelerator, using a thin gold target, and varied the maximum electron energy in 5-kev steps. Their results agree with the cross section as measured with radioisotope sources. They analyzed the bremsstrahlung spectrum using the Sauter-Fano theory, finding that this gave a better fit than did the earlier Bethe-Heitler theory. They attribute the peak reported in the earlier experiment to an incorrect analysis of the bremsstrahlung yield from the thick gold target used at that time.

A recent experiment at M.I.T. by Paolini (Pa60) determined the overall photoneutron spectrum from about 3 to 18 Mev. This is shown in Fig. 1. In this figure the peak just above threshold as determined with monoenergetic sources has been added to Paolini's results.

IV. THEORY

In 1949 Guth and Mullin (Gu49) calculated a theoretical cross section for photoneutron production in Be^9, based on a two-body model consisting of a single neutron loosely bound to a Be^8 core, and using square-well potentials. In their model the ground state is taken as a $P_{3/2}$ state. Electric dipole transitions then lead to an $S_{1/2}$ state near threshold and to $D_{3/2}$ and $D_{5/2}$ states at somewhat higher energies. The cross section for a magnetic dipole transition, which would lead to a $P_{1/2}$ state near threshold, was calculated to be very small. Their expression for the cross section for the P — S transition contains four adjustable parameters namely, the radius and depth of the initial and final wells. Making the assumption that the initial and final wells have the same radius of action and choosing the initial well depth to give the correct binding energy, reduces the number of adjustable parameters to two. For a given radius the depth of the final well is then chosen to result in a fit to the experimental cross section

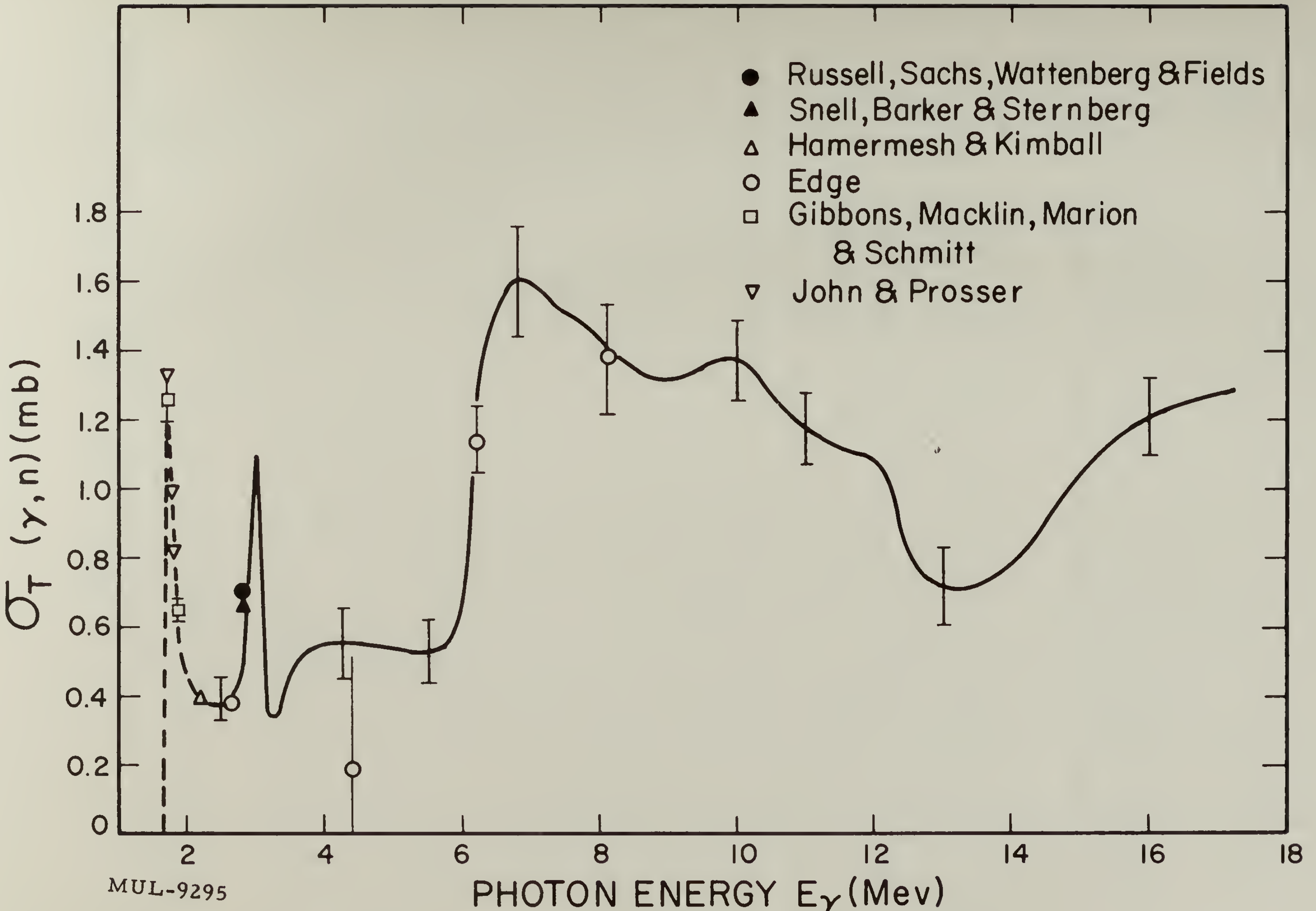

Fig. 1. $Be^9(\gamma,n)$ cross section (from Pa60).

near threshold. In their calculations they used a radius of 5.0 f (1 fermi $= 10^{-13}$ cm) and a final well depth of 3.0 Mev. The threshold (binding energy) at that time was thought to be 1.63 Mev. The total cross section calculated by Guth and Mullin is shown in Fig. 2.

An early theoretical treatment by Bergmann (Be51) was similar to that of Guth and Mullin, but the numerical results were different. Some of the data included in his paper indicated the effect of varying the parameters.

It appeared to us that the use of more recent experimental data, together with a judicious choice of parameters, might produce a better fit to the experimental cross section. On this basis, new square-well calculations following the treatment of Guth and Mullin were made. The detailed development of this theory is included in Appendix A of this report. Calculations were made using several values for the radius of the initial and final wells, and the initial well depth in each case was chosen to give the correct value of 1.666 Mev for the binding energy of the last neutron. The depth of the final well in each case was chosen for two different conditions: (1) correct energy dependence of the cross section, based on the experimental ratio of the cross section at 1.78 Mev to that at 1.692 Mev; and (2) correct value of the cross section at 1.692 Mev as experimentally determined. The results of these calculations are shown in Figs. 3 through 5, which also illustrate the effect of changing the various parameters. It is felt that, because of the magnitude of the parameters used to fit the experimental cross section, the square-well assumption is not entirely valid. The qualitative fit, however, is quite good, especially considering the simplicity of the model. It is interesting to note that the sharp peak just above threshold demands that the final state be a lightly bound state (~50 kev binding).

Goldman, Francis, and Guth (Go60) have recently calculated the theoretical cross section near threshold for the P − S transition using a single-particle shell model of the Saxon type:

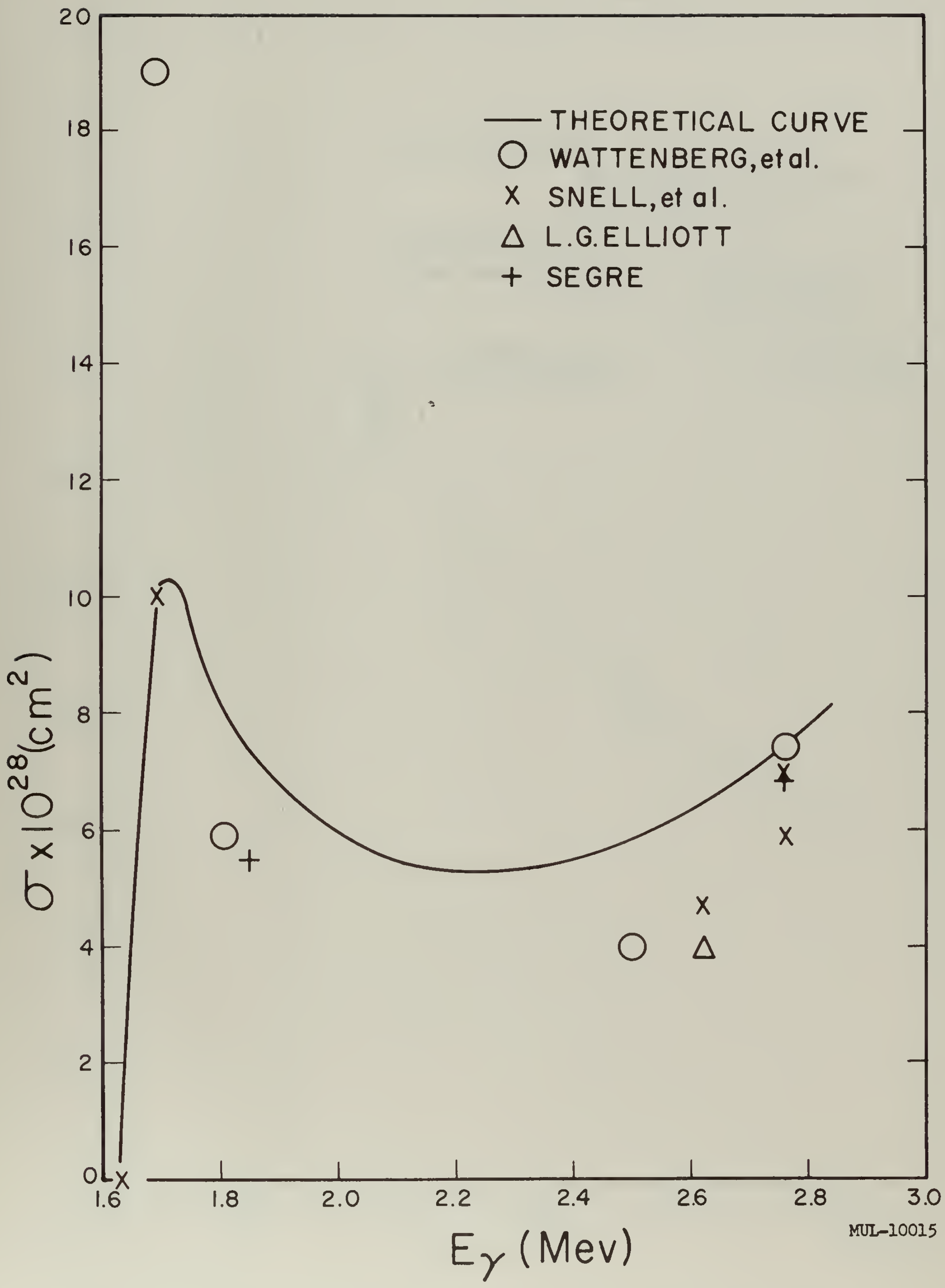

Fig. 2. $Be^9(\gamma, n)$ cross section (from Gu48).

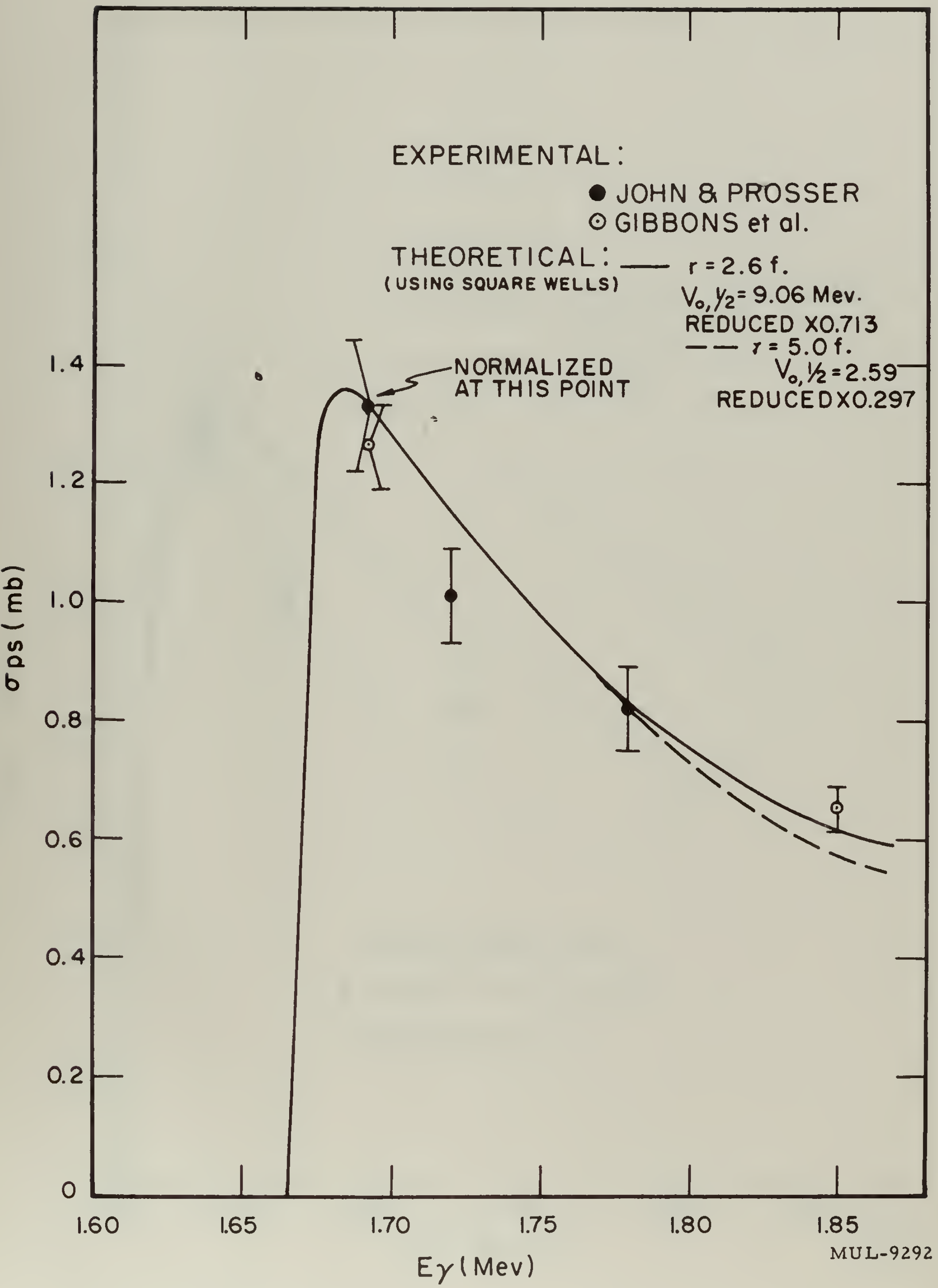

Fig. 3. $Be^9(\gamma,n)$ cross section curves illustrating the effect of varying r_0. $V_{0,1/2}$ is chosen to fit the ratio of the cross sections at 1.692 and 1.78 Mev. Note that the absolute magnitudes have been multiplied by reduction factors.

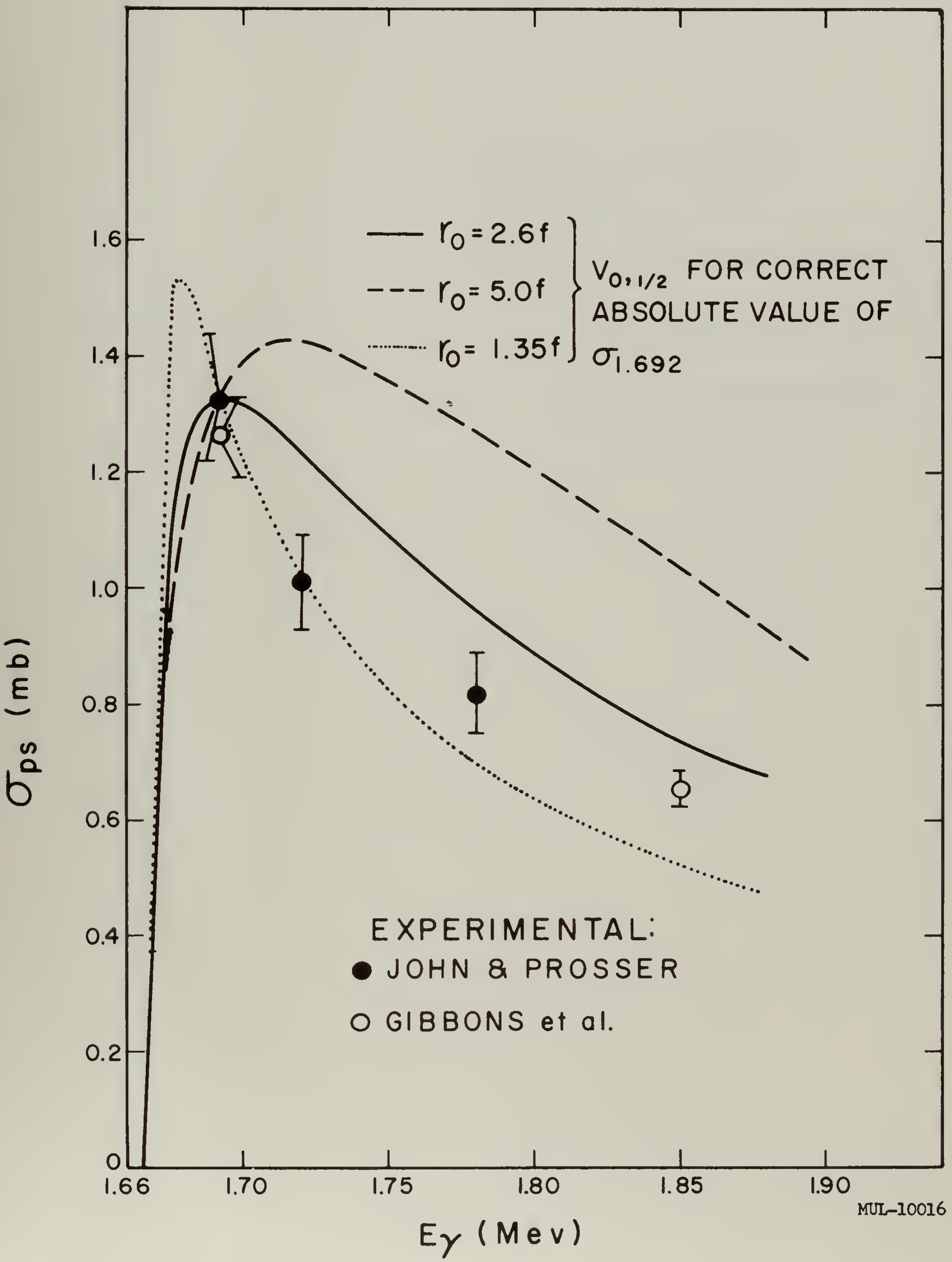

Fig. 4. For three values of r_0, $V_{0,1/2}$ has been chosen to fit the absolute value of the $Be^9(\gamma,n)$ cross section at 1.692 Mev.

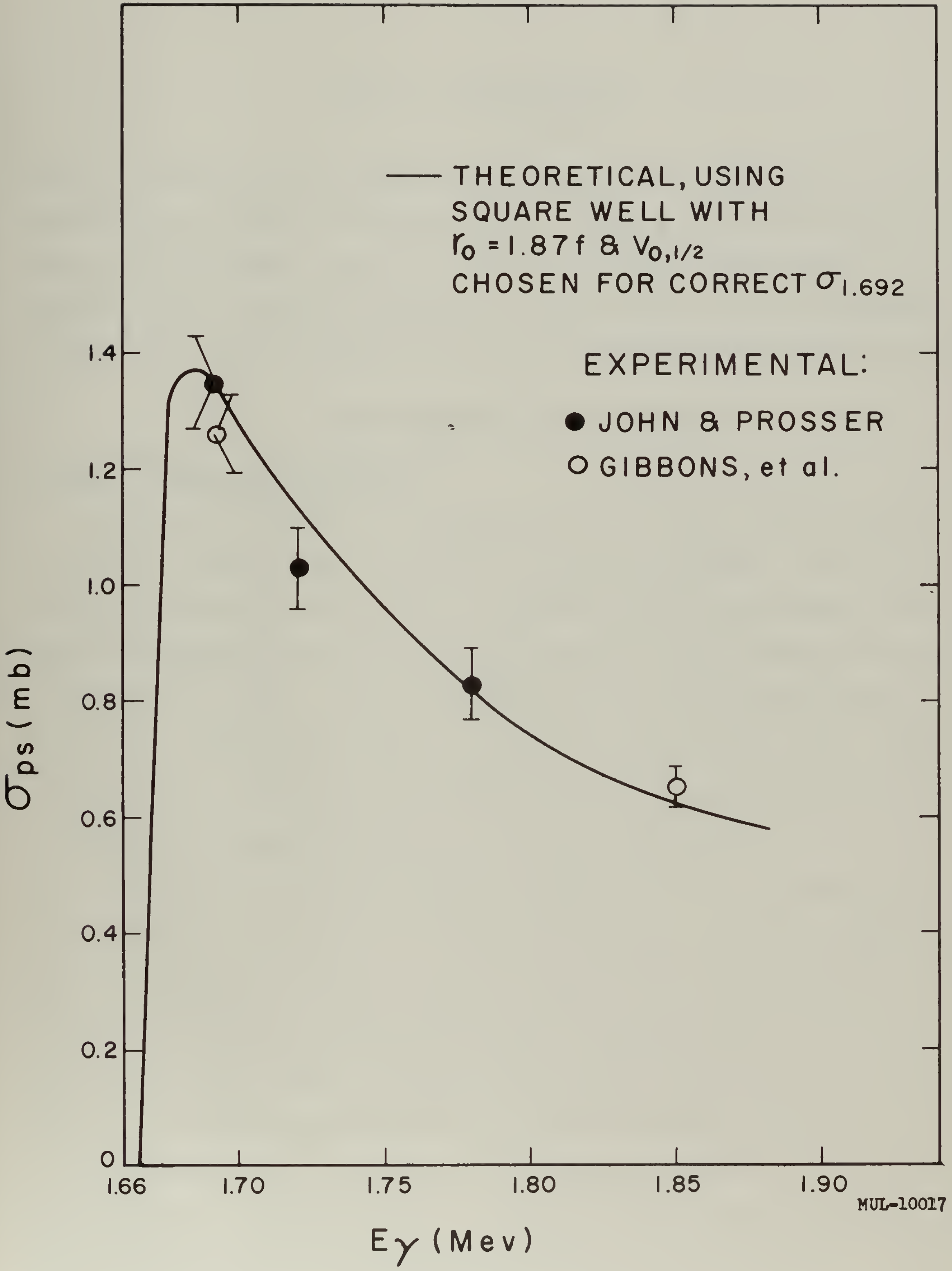

Fig. 5. The $Be^9(\gamma,n)$ cross section curve with r_0 and $V_{0,1/2}$ chosen to fit the absolute magnitude at 1.692 Mev and the ratio of the cross sections at 1.692 and 1.78 Mev.

$$V(r) = \frac{-V_0}{1 + \exp \frac{r-R}{a}}$$

with V_0 determined from the binding energy of the last neutron, and with the final well based on scattering data. Using R = 3.0f for both the initial and final states, with a = 0.6 f for the initial state and a = 1.2f for the final state, they have obtained a cross section curve which appears to fit the experimental data in both energy dependence and absolute magnitude.

V. EXPERIMENTAL PROCEDURE

A. Sb^{124} Gamma-Ray Source

It was decided that the total photoneutron cross section of Be^9 for the 1.692-Mev gamma rays from Sb^{124} would be measured. This was the closest gamma-ray energy to the threshold which was readily available in sufficient intensity and with a long enough half-life to permit convenient measurement. Also, this energy appears to be quite near the top of the peak in the cross section near threshold. Furthermore, Sb^{124} sources had been used in previous experiments (see Table I) which had resulted in cross section measurements differing by almost a factor of 2, and it was desired to clear up this long-standing discrepancy.

A source consisting of a hollow sphere of 1/16 in. aluminum packed with granulated antimony to a density of about 2.7 g/cm^3, and having a 1.36-cm outside diameter, was irradiated in the Livermore Pool Type Reactor (LPTR) to a total antimony activity of 225 millicuries and allowed to decay for a period of several months to eliminate any short-lived activity. This gamma-ray source was then held within a hollow beryllium sphere made up of nesting hemispheres, the whole assembly of beryllium having an outside diameter of 8.2 cm and a thickness of 0.645 cm. A sketch of the assembly is shown in Fig. 6. The particular source geometry used was chosen to: (1) give spherical symmetry; (2) minimize the correction necessary for the finite size of the Sb^{124} source; and (3) reduce the absorption of gamma rays and the moderation of neutrons in the beryllium shell to a reasonable amount.

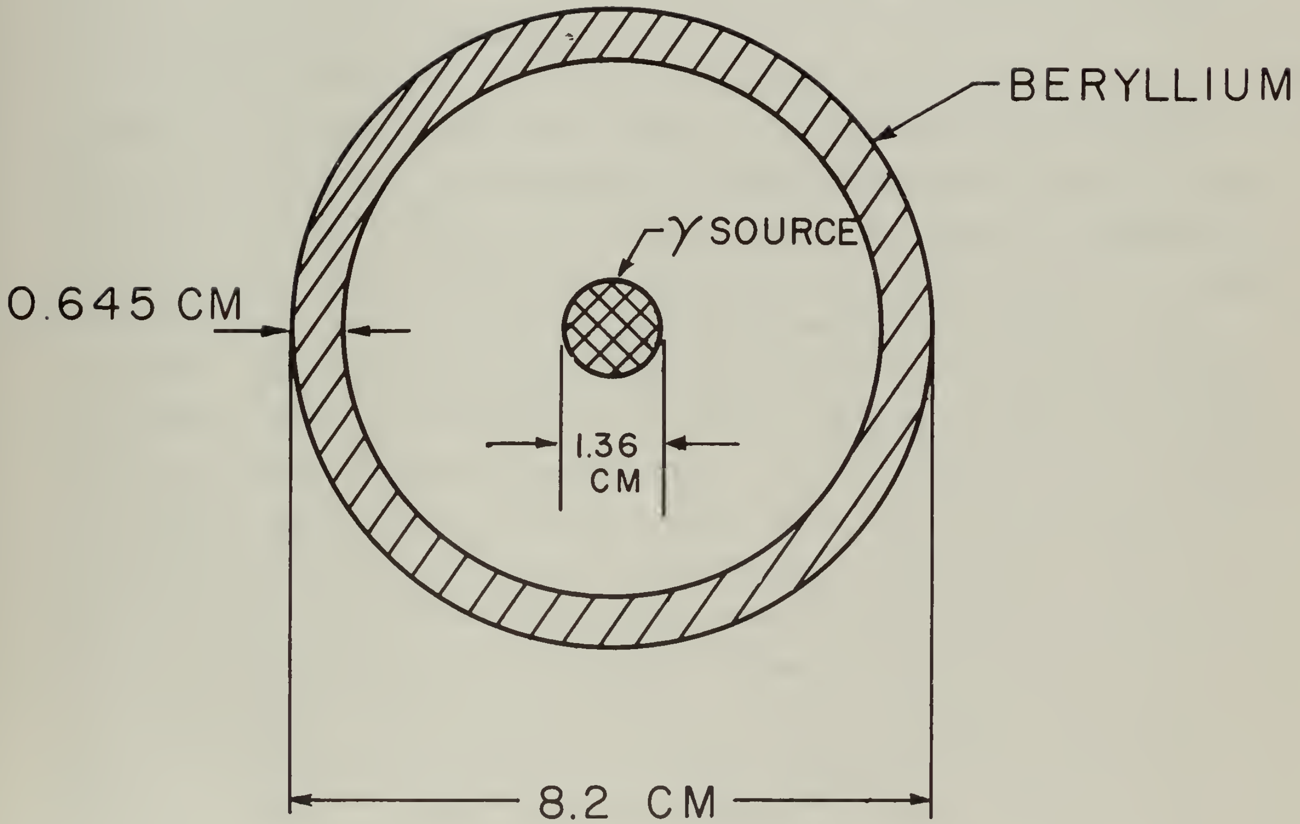

Fig. 6. Beryllium photoneutron source. MUL-8456

B. Neutron Counting

In order to measure the neutron flux, a long counter was constructed following the pattern of the Harwell 4 model (Al55). The effective face of the counter was determined by using Po-Be, Pu-Be, Po-Li, Sb-Be, and mock fission sources at various distances, and plotting (count rate)$^{-1/2}$ vs distance from the actual face of the counter. The use of the long counter for absolute neutron flux measurements proved unsatisfactory, however, because of the different geometries of the various sources and an uncertainty as to the variation in efficiency of the counter over such a broad range of neutron energies.

As a better means of counting the total neutron flux, a manganous sulfate bath was prepared (Ge59). This method of determining neutron flux has the advantage that essentially all the neutrons are moderated and captured by the manganese, so that the resulting activation is independent of the neutron energy spectrum. A tank 44 in. in diameter and 29 in. deep was filled with a nearly saturated solution of manganous sulfate, using 175 gallons of distilled water in which was dissolved 575 pounds of $MnSO_4$. A Victoreen 1B85 Geiger-Muller tube was attached to a probe of aluminum tubing and waterproofed for dip counting. A Cs^{137} button source was fixed in a standard geometry for periodic checks of the G-M tube counting rate. An NBS Ra-Be source was used to calibrate the $MnSO_4$ bath. It was suspended in the center of the tank in a waterproof holder made of aluminum and the bath was activated to saturation. Since the half-life of Mn^{56} is 2.58 hours, any activation over a period of a day or longer essentially saturates the bath. The G-M tube was then placed in the center of the bath and a series of counts taken over a period of several half-lives of the Mn^{56} to ensure that the proper activity was being counted. From the results of this series of counts, the count rate at the time of removal of the source from the bath was computed. From this initial counting rate and the total flux of the NBS source, the total flux of any other neutron source can be determined by immersing it in the bath and activating the bath to saturation. The ratio of the fluxes is then the same as the ratio of the initial counting rates. The initial counting rate obtained with the

NBS source has proved to be reproducible to within 1% in subsequent measurements. This procedure was followed in determining the total neutron flux produced by the antimony-beryllium source assembly.

C. Strength of Gamma-Ray Source

In order to compute the photoneutron cross section, it was necessary that the total flux of gamma-ray photons with an energy of 1.692 Mev be determined. This was accomplished by the use of a thallium-activated sodium-iodide scintillation crystal and a 256-channel pulse-height analyzer. Computations of the gamma-ray intensity were based on unpublished curves for intrinsic crystal efficiency and photofraction furnished by Harry West of this laboratory. It is estimated that the accuracy of this method is better than 5%. The scintillation counting technique is felt to be the best method of determining the strength of the gamma-ray source in this experiment, since it is independent of the decay scheme of the source, and provides an automatic correction for self-absorption and Compton scattering in the source. In using other methods the strength of a particular gamma line must be calculated from a knowledge of the decay scheme involved, and in many instances the decay scheme is not known with great accuracy. With the scintillator and pulse-height analyzer combination, only those gamma rays that have a specific energy are counted, and further, any gamma rays absorbed in the source are not counted, just as they are not seen by the beryllium surrounding the gamma-ray source. In addition, any gamma rays which are Compton scattered are not counted under the photopeak. This is desirable, in the case of antimony, since almost all (99.5%) of those photons which have undergone Compton scattering are below the threshold for photodisintegration. Thus the gamma-ray source looks the same to the scintillator as it does to the beryllium, and corrections for absorption and Compton scattering are applied automatically, giving a more accurate evaluation of the gamma-ray flux available to produce photoneutrons.

D. Computation of Cross Section

Once the gamma-ray flux (at the required energy) and the neutron flux are known, the total cross section for photoneutron production at the particular energy involved can be computed from

$$\sigma = \frac{N_n A_{Be}}{N_\gamma N_0 \rho_{Be} \Delta r} ,$$

where

σ = cross section in cm^2

N_n = neutron flux in neutrons/sec

A_{Be} = atomic weight of Be^9

N_γ = gamma-ray flux in photons/sec

N_0 = Avogadro's number

ρ_{Be} = density of Be^9 in g/cm^3

Δr = thickness of Be^9 shell in cm.

E. Comparison Technique

It was desired to explore the photoneutron cross section near threshold in as much detail as possible using radioisotopes, but the gamma-ray sources available in this energy region are limited to a few which have short half-lives and/or low intensities. With a half-life less than several hours or a total neutron flux less than about 10^4 n/sec, the use of the $MnSO_4$ bath becomes subject to large uncertainties. Therefore, a new experimental arrangement providing for the following considerations was desirable:

1. The measurement should be independent of half-life. This could be accomplished by a simultaneous count of gamma rays and neutrons.

2. It should be possible to count a weak neutron flux. This could be done with a long counter.

3. The effect of room scattered neutrons should be minimized. This could be done by placing the source close to the long counter.

4. Since there are about 10^4 gamma photons for each neutron produced, and since the scintillation counter is more efficient than the long

counter, precautions must be taken to prevent excessive gamma counting rates, with attendant dead-time losses. This requirement could be satisfied by locating the scintillator at a distance from the source, and by using a collimator at the crystal as necessary.

The arrangement finally devised is shown in Fig. 7. The simultaneous count of neutrons and gammas results in an n/γ ratio which is proportional to the cross section. When several gamma sources of different energies are used successively in the same geometry, a relative cross section curve is readily obtained. This can then be converted to an absolute cross section curve if the correct aboslute value is known at one of the energies.

In computing the n/γ ratios, corrections are made for the variation in intrinsic efficiency and photofraction of the NaI scintillator. No corrections were made for variations in efficiency of the long counter. This counter was of the Harwell 4 type which Allen found to be flat down to Sb-Be photoneutron energy (Al 55). Even for the typical 10-15% droop of the efficiency of a long counter, our efficiency uncertainty would not be greater than about 2%. The long counter was biased to eliminate γ counting.

This comparison technique was used to make cross-section measurements at 1.78 Mev with Al^{28} as the gamma-ray source, and at 1.72 Mev with Bi^{206}. A sphere of solid aluminum the same size as the antimony source was activated in the LPTR and placed in the center of the beryllium shell. It was necessary to work rapidly, since the half-life of Al^{28} is only 2.3 minutes. This was accomplished by removing the source from the reactor by a pneumatic tube delivery system, so that the total elapsed time after removal from the reactor flux until the count of the Al-Be assembly was started was less than one half-life. A lead collimator having a 3/4-in. aperture was used at the scintillation crystal to cut down the counting rate for the gamma rays while still maintaining a good neutron counting rate. Several successive runs were made as the source decayed, and those runs having good counting rates without excessive dead-time corrections were used in computing the n/γ ratio. The n/γ ratio for

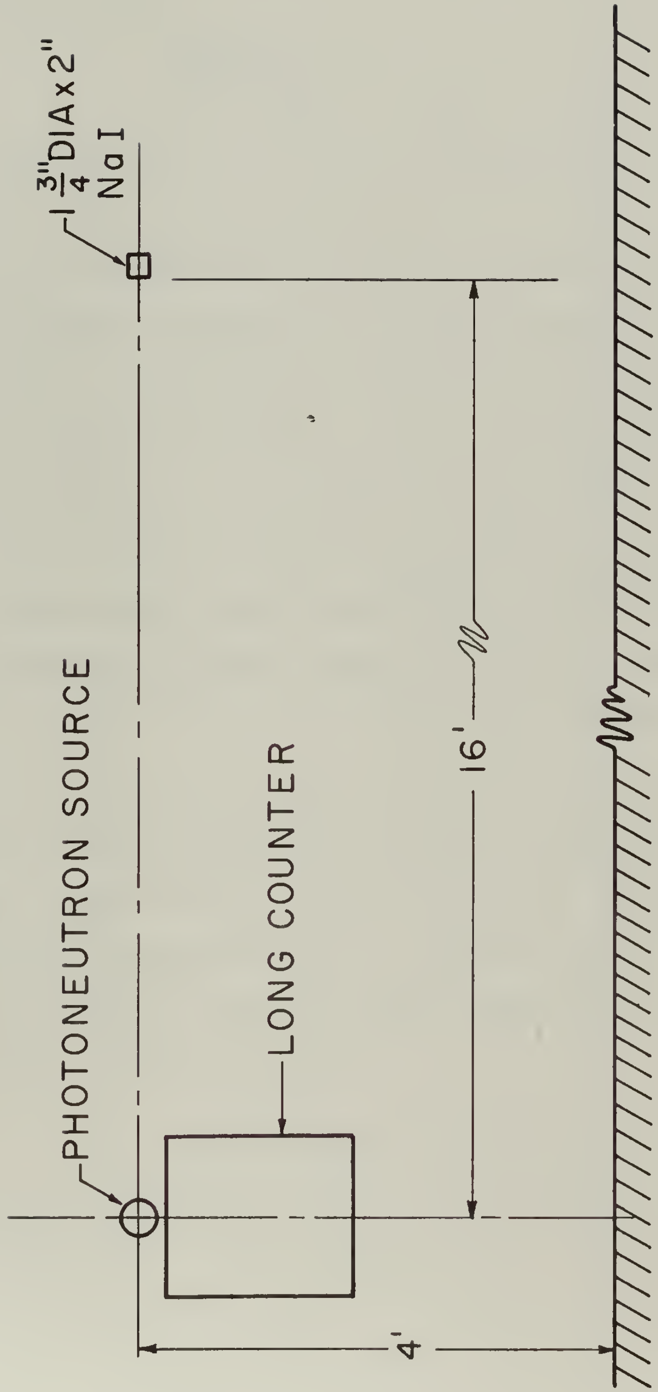

MUL-8455

Fig. 7. Experimental arrangement for comparison technique.

antimony in the same geometry was measured and the cross section at 1.78 Mev computed by

$$\frac{(n/\gamma)_{1.78}}{(n/\gamma)_{1.692}}\,\sigma_{1.692} = \sigma_{1.78}\,.$$

It should be noted that the ratio of the cross sections is considerably more accurate than the absolute value.

For the measurement at 1.72 Mev a foil of high-purity lead was bombarded in the 60-inch cyclotron at Berkeley to produce the reaction Pb^{206} (d, 2n) Bi^{206}. The procedure was then the same as that used in the case of the aluminum source, except that the bismuth source was considerably weaker, so the collimator was not used at the scintillation crystal. The ratio n/γ for the bismuth source was somewhat more difficult to determine than for either the aluminum or the antimony, since some Bi^{205} was present from the Pb^{206} (d, 3n) Bi^{205} reaction. A rather complex gamma-ray spectrum resulted from this contamination, and it was necessary to separate out its effect on the basis of pulse height and half-life.

There are several other radioisotopes with gamma-ray energies above threshold and short half-lives which could be used in this comparison technique. We know of no others, however, which have gamma-ray energies between threshold and the 1.78 Mev from the Al^{28}. Use of higher energies than this would probably demand an individual calibration of the long counter efficiency curve.

VI. EXPERIMENTAL RESULTS

In measuring the photoneutron cross section at 1.692 Mev, using gamma rays from Sb^{124}, the following results were obtained:

Strength of NBS Ra-Be source E-1277 as of 9 December 1954:

$$Q_0 = (6.09 \pm 3\%) \times 10^6 \text{ n/sec.}$$

Strength as of 17 September 1959 considering growth of Po^{210}:

$$Q = Q_0 \left[1.12 - 0.12 \exp(-t/28)\right]$$
$$= (6.21 \pm 3\%) \times 10^6 \text{ n/sec.}$$

$(dN/dt)_0$ for NBS source in $MnSO_4$ bath = 1292 c/min

$(dN/dt)_0$ for Sb-Be source assembly = 11.05 c/min

N_n from Sb-Be $= \frac{11.05}{1292} \times 6.21 \times 10^6 = 5.31 \times 10^4$ n/sec

N_γ for 1.692-Mev line of Sb^{124} as of 3 September 1959 $= 5.61 \times 10^8$

N_γ as of 17 September 1959 $= 5.61 \times 10^8 \exp(-0.693 \times 14/60.9)$

$= 4.78 \times 10^8$ photons/sec

The following corrections and uncertainties apply:

Correction to cross section	Correction (%)	Uncertainty(%)
Gamma-ray source strength	---	5.0
Neutron counting statistics	---	2.0
Finite source size	−0.3	< 0.1
Attenuation of gamma ray in Be shell	+2.5	< 0.1
Effect of 2.09-Mev gamma ray	−4.4	1.0
Neutron escape from $MnSO_4$ bath	−0.9	< 0.1
Absolute strength of NBS source E−1277	---	3.0
Total correction	−3.1	---
Overall uncertainty	---	6.2

The corrections for finite source size, attenuation of the gamma ray in the Be shell, effect of the 2.09-Mev gamma-ray, and neutron escape from the $MnSO_4$ bath are described in Appendix B.

The cross section is now computed as follows:

$$\sigma = \frac{N_n A_{Be}}{N_\gamma N_0 \rho_{Be} \Delta r} (1 - 0.031)$$

$$= \frac{5.32 \times 10^4 \times 9.02 \times 0.969}{4.78 \times 10^8 \times 6.025 \times 10^{23} \times 1.85 \times 0.645}$$

$$= 1.35 \times 10^{-27} \text{ cm}^2$$

$$\sigma = 1.35 \pm 0.08 \text{ mb} .$$

In determining the cross section at 1.78 Mev the comparison technique described previously was used, with Al^{28} as the source of gamma rays, and the following results were obtained:

n/γ for Sb-Be = 0.1179

$$n/\gamma \text{ for Al-Be} = 0.0728$$

$$\sigma_{1.78} = \frac{0.0728}{0.1179} \times 1.35 = 0.83 \text{ mb} .$$

The ratio of the cross sections at 1.78 Mev and 1.692 Mev is considered to be much more accurate than the absolute value of the cross section, having an estimated uncertainty of ± 2%. This gives an overall uncertainty at 1.78 Mev of 6.6%, so that

$$\sigma_{1.78} = 0.83 \pm 0.06 \text{ mb} .$$

In the case of the cross section at 1.72 Mev, the strength of the Bi^{206} gamma-ray source was rather low, so the collimator was removed from the sodium iodode crystal to obtain better gamma counting statistics. This change in geometry changed the n/γ ratio for the Sb-Be assembly. The following results were obtained:

$$n/\gamma \text{ for Sb-Be} = 0.0421$$

$$n/\gamma \text{ for Bi-Be} = 0.0309 .$$

From these figures a preliminary cross section at 1.72 Mev was computed as

$$\sigma_{1.72} \cong \frac{0.0309}{0.0421} \times 1.35 = 0.991 \text{ mb} .$$

It was necessary to make an additional correction to this preliminary value, since there was an appreciable amount of Bi^{205} present in the source. Bi^{205} has strong gamma rays at energies of 1.766 and 1.777 Mev. These, together with the 1.72-Mev gamma ray from the Bi^{206}, resulted in a broad photopeak made up of one peak at 1.72 Mev and another, approximately one-fourth as intense, at about 1.77 Mev. Even if the ratio of the two peaks were 1:3 or 1:5 rather than the estimated ratio of 1:4, the resulting cross section would not change by more than about 1.3%. The assumption of a cross section of 0.85 mb as a reasonable value of 1.77 Mev leads to

$$0.8\sigma_{1.72} + 0.2\ (0.85) = 0.991 \text{ mb};$$

so that

$$\sigma_{1.72} = 1.03 \text{ mb} .$$

Because of the complicated spectrum, an uncertainty of ± 3% was estimated for the comparison procedure in this case. This leads to

an overall uncertainty of about 7% for the cross section at 1.72 Mev, with the result that

$$\sigma_{1.720} = (1.03 \pm 0.07) \text{ mb} .$$

In regard to the absolute value of the cross section, it should be mentioned that the antimony source was also counted by the Hazards Control Group using a Landswerk Condenser R-meter. The total strength of the source was measured as 47.5 mc as of 11 August 1959. The strength as of 17 September 1959 was then 31.2 mc. If we assume that the 1.692-Mev gamma ray occurs in 50.6% of the disintegrations (Gi59), the strength of this gamma ray was 5.84×10^8 photons/sec. This must be corrected for scattering within the source, since scattered gammas are counted by the R-meter but are below the photoneutron threshold. The correction is about 6.5%, so that

$$N_\gamma = 5.46 \times 10^8 \text{ photons/sec} .$$

Subsituting this value in the cross section formula we obtain

$$\sigma = 1.18 \pm 0.07 \text{ mb} .$$

As stated previously, it is felt that this method of measurement is not as reliable as that using the scintillation crystal. However, the difference in the values obtained by the two methods indicates the presence of some systematic error, possibly in the branching ratio.

In an attempt to improve the accuracy of the original cross section measurement at 1.692 Mev, particularly the neutron counting statistics, a stronger antimony source has been prepared and the neutron flux measured. This source was also counted by the Hazards Control Group. Their measurement of the stronger source leads to the same cross section, within 1%, as did their measurement of the earlier source. The estimated uncertainty for the neutron counting statistics as shown in the table of corrections to the cross sections is based on the measurement of this stronger source. Even though the cross section based on scintillation spectrometry is considered more accurate than that based on R-meter measurements, the latter have proved consistent in successive measurements of an antimony source, within the known accuracy of the half-life.

VII. CONCLUSIONS

The value obtained in the present experiment for the photoneutron cross section at 1.692 Mev is in reasonable agreement with the recent accurate determination by Gibbons et al. (Gi59). This agreement removes the long-standing large uncertainty in the value of the cross section at 1.692 Mev.

The energy dependence of the cross section near threshold is now well defined by the combination of our results at 1.692, 1.720, and 1.78 Mev with the data of Gibbons et al. (Gi59) and Walter et al. (Wa60).

The use of a square-well potential in the theory of Guth and Mullin does not give a fit to the data unless the radius is made unrealistically small (1.87f). The new calculation by Goldman et al. (Go60) using a Saxon-Woods potential with reasonable parameters results in a good fit to the experimental data.

VIII. ACKNOWLEDGMENTS

The authors wish to express their appreciation to F. J. Lombard, Jr., E. T. Moore, and M. J. Schwartz for their work in the early stages of the experiment, to J. L. Minkler for counting the antimony sources, to H. I. West, Jr., for the crystal efficiency and photofraction curves, and to W. A. Sherwood for the numerical calculations of the theoretical cross section. Appreciation is also due to A. J. Kirschbaum and J. E. Carothers for their continued interest and support throughout the experiment, and to the LPTR staff for invaluable help in source preparation and instrumentation. We are also indebted to D. T. Goldman, N. C. Francis, E. Guth, R. L. Walter, M. F. Shea, W. C. Miller, and P. T. Demos for communicating results to us before publication.

This work was performed under the auspices of the U. S. Atomic Energy Commission.

REFERENCES

(Al50) D. L. Allen and M. J. Poole, Nature 162, 373 (1950).

(Al52) D. E. Alburger, Phys. Rev. 88, 1257 (1952).

(Al55) W. D. Allen, A.E.R.E. NP/R 1667 (1955).

(Be51) O. Bergmann, Acta Phys. Austriaca 4, 338 (1951).

(Bi50) Bishop, Collie, Halban, Hedgran, Siegbahn, DuToit, and Wilson, Phys. Rev. 80, 211 (1950).

(Ch34) J. Chadwick and M. Goldhaber, Nature 134, 237 (1934).

(Co56) D. R. Connors and W. C. Miller, Bull. Am. Phys. Soc. 1, 340 (1956).

(Ed56) R. D. Edge, Nuclear Phys. 2, 485 (1956).

(Ge59) K. W. Geiger and G. N. Whyte, Can. J. Phys. 37, 256 (1959).

(Gi59) J. H. Gibbons, R. L. Macklin, J. B. Marion, and H. W. Schmitt, Phys. Rev. 114, 1319 (1959).

(Go60) D. T. Goldman, N. C. Francis, and E. Guth, Bull. Am. Phys. Soc. 5, 45 (1960); also private communication.

(Gu49) E. Guth and C. J. Mullin, Phys. Rev. 76, 234 (1949).

(Ha53) B. Hamermesh and C. Kimball, Phys. Rev. 90, 1063 (1953).

(Pa60) F. R. Paolini, Doctoral Thesis, M.I.T. (1960) (unpublished).

(Ru48) B. Russell, D. Sachs, A. Wattenberg, and R. Fields, Phys. Rev. 73, 545 (1948).

(Sn50) A. H. Snell, E. C. Barker, and R. L. Sternberg, Phys. Rev. 80, 637 (1950).

(Sz34) L. Szilard and T. A. Chalmers, Nature 134, 494 (1934).

(Wa60) R. L. Walter, M. F. Shea, and W. C. Miller, Bull. Am. Phys. Soc. 5, 229 (1960); also private communication.

APPENDIX A
THEORETICAL DEVELOPMENT USING SQUARE-WELL POTENTIALS

This development follows that of Guth and Mullin (Gu48) but is presented in more detail. We considered it necessary to verify the formulae of Guth and Mullin because of the different numerical results obtained by Bergmann (Be51).

The general formula for the electric dipole photoneutron cross section is

$$\sigma = \frac{8\pi^3\nu}{c} \sum_{1} \left|M_z(E)\right|^2 \tag{1}$$

in which

$$M_z(E) = Ze\frac{\mu}{m} \int \psi_f^* z\, \psi_i\, d\tau. \tag{2}$$

μ/m is the ratio of the reduced mass of the system to the mass of the residual nucleus, $z = r\cos\theta$ is the electric dipole operator, and $E = h\nu - \epsilon$, where ϵ is the binding energy of the neutron to the residual nucleus.

Using a ground P state, the selection rule $\Delta l = \pm 1$ for electric dipole transitions permits P → S and P → D transitions. Only the P → S transition will be treated here, since it is the one which is important near threshold.

The expression for the electric dipole disintegration of Be^9 then becomes

$$\sigma = \frac{8\pi^3\nu}{c}\left(\frac{4}{9}e\right)^2 \sum \left|\int \psi_f^* z\, \psi_i\, d\tau\right|^2 , \tag{3}$$

where the summation extends over all non-vanishing matrix elements. Assuming the spin interaction to be small and of a central (non-tensor) type, the eigenstates f, i are described by the quantum numbers E (energy), j, m_j, and l. The eigenfunctions are

$$\psi\,(l,\ j = l + \tfrac{1}{2},\ m_j) = \frac{R_{l,\,j}(r)}{(2l+1)^{1/2}} \Big[(l + \tfrac{1}{2} + m_j)^{1/2}\, Y_{l,\,m_j - \frac{1}{2}}\,(\theta,\phi)\,\alpha_n$$

$$+ (l + \tfrac{1}{2} - m_j)^{1/2}\, Y_{l,\,m_j + \frac{1}{2}}\,(\theta,\phi)\,\beta_n \Big] \qquad (4a)$$

$$\psi\,(l,\ j = l - \tfrac{1}{2},\ m_j) = \frac{R_{l,\,j}(r)}{(2l+1)^{1/2}} \Big[(l + \tfrac{1}{2} - m_j)^{1/2}\, Y_{l,\,m_j - \frac{1}{2}}\,(\theta,\phi)\,\alpha_n$$

$$- (l + \tfrac{1}{2} + m_j)^{1/2}\, Y_{l,\,m_j + \frac{1}{2}}\,(\theta,\phi)\,\beta_n \Big] \qquad (4b)$$

The matrix element $\int \psi_f^* \, z \, \psi_i \, d\tau$ of Eq. (3) is different from zero only if $\Delta l = \pm 1$, $\Delta j = 0, \pm 1$, and $\Delta m_j = 0$. α_n and β_n are spin operators with the property that $\alpha_n^* \alpha_n = \beta_n^* \beta_n = 1$ and $\alpha_n^* \beta_n = \beta_n^* \alpha_n = 0$.

For a $P_{3/2}$ initial state, m_j can be ± 3/2 or ± 1/2 with equal probability. Since the final $S_{1/2}$ state can only have $m_j = \pm 1/2$, a factor of 1/2 in the final cross section results from the selection rule $\Delta m_j = 0$. Furthermore, Eq. (4b) would apply to a $P_{1/2}$ state, so that only Eq. (4a) need be considered in the case of a $P_{3/2}$ initial state.

Considering $m_j = +1/2$, the initial eigenfunction is

$$\psi\,(1,\ 3/2,\ +1/2) = \frac{R_{1,\,3/2}(r)}{(3)^{1/2}} \left[(2)^{1/2}\, Y_{1,0}(\theta,\phi)\,\alpha_n + Y_{1,1}(\theta,\phi)\,\beta_n \right]. \qquad (5a)$$

For $m_j = -1/2$, the initial eigenfunction is

$$\psi\,(1,\ 3/2,\ -1/2) = \frac{R_{1,\,3/2}(r)}{(3)^{1/2}} \left[Y_{1,\,-1}(\theta,\phi)\,\alpha_n + (2)^{1/2}\, Y_{1,0}(\theta,\phi)\,\beta_n \right]. \qquad (5b)$$

For $m_j = +1/2$, the final eigenfunction is

$$\psi\,(0,\ 1/2,\ +1/2) = R_{0,\,1/2}(r) \left[Y_{0,0}\,(\theta,\phi)\,\alpha_n \right]. \qquad (5c)$$

For $m_j = -1/2$, the final eigenfunction is

$$\psi\,(0,\ 1/2,\ -1/2) = R_{0,1/2}(r) \left[Y_{0,0}(\theta,\phi)\,\beta_n \right]. \qquad (5d)$$

The expression $\int \psi_f^* \, z \, \psi_i \, d\tau$ can now be written as

$$(2/3)^{1/2} \iiint \left(R_{0,1/2}^*\, Y_{0,0}^* \right) r \cos\theta \left(R_{1,3/2}\, Y_{1,0} \right) r^2 \sin\theta \, dr \, d\theta \, d\phi$$

Separating variables gives

$$(2/3)^{1/2} \int R^*_{0,\,1/2}\, R_{1,\,3/2}\, r^3\, dr \iint Y^*_{0,\,0}\, Y_{1,\,0} \cos\theta \sin\theta \, d\theta \, d\phi \,.$$

The normalized spherical harmonics are

$$Y_{0,\,0} = \left(\frac{1}{4\pi}\right)^{1/2} \qquad Y_{1,\,0} = \left(\frac{3}{4\pi}\right)^{1/2}$$

which results in

$$\frac{(2)^{1/2}}{4\pi} \int R^*_{0,\,1/2}\, R_{1,\,3/2}\, r^3\, dr \iint \cos^2\theta \sin\theta \, d\theta \, d\phi \,.$$

Integrating the angle part gives

$$\left(\frac{2}{3}\right)^{1/2} \int R^*_{0,\,1/2}\, R_{1,\,3/2}\, r^3\, dr \,.$$

Considering the factor of 1/2 mentioned previously, the expression

$$\sum \left| \int \psi_f^* \, z \, \psi_i \, d\tau \right|^2$$

now becomes

$$\frac{1}{2} \left[\left(\frac{2}{3}\right)^{1/2} \right]^2 \left| R_{ps} \right|^2 = \frac{1}{9} \left| R_{ps} \right|^2 ,$$

where

$$R_{ps} = \int_0^\infty R^*_{0,1/2}\, R_{1,\,3/2}\, r^3\, dr \,.$$

This makes the expression for the cross section

$$\sigma = \frac{128\pi^3}{729} \frac{e^2}{c} \nu \left| R_{ps} \right|^2 .$$

By using $h\nu = \hbar\omega$ and $h = 2\pi\hbar$, this becomes

$$\sigma = \frac{64\pi^2}{729} \frac{e^2}{\hbar c} \hbar\omega \left| R_{ps} \right|^2 . \qquad (7)$$

The only remaining problem is the evaluation of R_{ps}. Using the spherical square-well potential, for the initial state

$$V = -V_{1,\,3/2} \qquad r \le r_0$$

$$V = 0 \qquad r \ge r_0$$

and the radial wave functions are

$$R_{1,\,3/2} = A_1 j_1 (\beta r) \qquad r \le r_0$$

$$= A_1 \left(\frac{\sin \beta r}{(\beta r)^2} - \frac{\cos \beta r}{\beta r} \right)$$

$$R_{1,3/2} = B_1 \frac{1+\alpha r}{r^2} e^{-\alpha(r-r_0)} \qquad r \geq r_0 .$$

where

$$\alpha = \left[\frac{2\mu}{\hbar^2} \epsilon\right]^{1/2}$$

and

$$\beta = \left[\frac{2\mu}{\hbar^2}(V_{1,3/2} + E)\right]^{1/2}$$

with μ = reduced mass of neutron = $\frac{8M}{9}$.

Matching the logarithmic derivative $\frac{1}{R}\frac{dR}{dr}$ at $r = r_0$ gives

$$B_1 = -\frac{A_1}{\alpha^2} \sin \beta r .$$

$$\beta r_0 \cot \beta r_0 = 1 + (1 + \alpha r_0)\left(\frac{\beta}{\alpha}\right)^2 .$$

Normalizing by using $\int_0^\infty (R_{1,3/2})^2 r^2 dr = 1$ gives

$$\frac{A_1^2 r_0}{2\beta^2} \left\{1 + \left[(2 + \alpha r_0)\left(\frac{\beta}{\alpha}\right)^4 + (1 + \alpha r_0)\left(\frac{\beta}{\alpha}\right)^2 - 1\right] \frac{\sin^2 \beta r_0}{(\beta r_0)^2}\right\} = 1 .$$

For the final $S_{1/2}$ state, assuming the same radius of action for the initial and final states

$$V = -V_{0,1/2} \qquad r \leq r_0$$

$$V = 0 \qquad r \geq r_0$$

The radial wave functions for this state are then

$$R_{0,1/2} = A_0 j_0 (\gamma r) \qquad r \leq r_0$$

$$= A_0 \frac{\sin \gamma r}{\gamma r}$$

$$R_{0,1/2} = B_0 \frac{\sin\left[k(r - r_0) + \delta_0\right]}{kr} \qquad r \geq r_0$$

where

$$\gamma = \left[\frac{2\mu}{\hbar^2}(V_{0,1/2} + E)\right]^{1/2}$$

and $$k = \left(\frac{2\mu}{\hbar^2} E\right)^{1/2}$$

It will be noted that the wave function for $r \geq r_0$ is that for a free particle with phase shift δ_0.

Matching the logarithmic derivative at $r = r_0$ leads to

$$A_0 \sin \gamma r_0 = \frac{\gamma}{k} B_0 \sin \delta_0$$

$$A_0 \cos \gamma r_0 = B_0 \cos \delta_0 .$$

The normalization in this case is not so straightforward as for the initial state. It is accomplished as follows:

$$\int_0^\infty (R_{0,\,1/2})^2 r^2 \, dr = 1 \tag{8}$$

$$A_0^2 \int_0^{r_0} \left[j_0 (\gamma r) \right]^2 r^2 \, dr + B_0^2 \int_{r_0}^\infty \left\{ \frac{\sin\left[k(r - r_0) + \delta_0\right]}{kr} \right\}^2 r^2 \, dr = 1.$$

The first integral is readily integrated:

$$A_0^2 \int_0^{r_0} \left[\frac{\sin \gamma r}{\gamma r} \right]^2 r^2 \, dr = \frac{A_0^2}{2\gamma^3} \left[\gamma r_0 - \cos \gamma r_0 \sin \gamma r_0 \right] .$$

To integrate the second integral, assume for the moment a small energy spread such that $dk = (k_1 - k_2) << 1$ and write the integral

$$B_0^2 \int_{r_0}^\infty \left\{ \frac{\sin\left[k_1 (r - r_0) + \delta_0\right]}{k_1 r} \quad \frac{\sin\left[k_2 (r - r_0) + \delta_0\right]}{k_2 r} \right\} r^2 \, dr .$$

For the upper limit, substitute g and rewrite as

$$\frac{B_0^2}{k_1 k_2} \lim_{g \to \infty} \int_{r_0}^g \sin\left[k_1 (r - r_0) + \delta_0\right] \sin\left[k_2 (r - r_0) + \delta_0\right] dr .$$

Now substitute $x = r - r_0$, giving

$$\frac{B_0^2}{k_1 k_2} \lim_{g \to \infty} \int_0^g \sin (k_1 x + \delta_0) \sin (k_2 x + \delta_0) \, dx .$$

This can now be integrated to give

$$\frac{B_0^2}{k_1 k_2} \lim_{g \to \infty} \left\{ \frac{\sin (k_1 - k_2) g}{2 (k_1 - k_2)} - \frac{\sin \left[(k_1 + k_2) g + 2 \delta_0 \right]}{2 (k_1 + k_2)} \right\} .$$

Now, since $(k_1 - k_2) << 1$, all terms resulting from the left side of Eq. (8) are negligible except

$$\frac{B_0^2}{k_1 k_2} \lim_{g \to \infty} \left[\frac{\sin (k_1 - k_2) g}{2(k_1 - k_2)} \right] .$$

This can be rewritten in terms of the Dirac delta function as follows (see L. I. Schiff, Quantum Mechanics, McGraw-Hill, 1959, p. 51):

$$\frac{B_0^2}{k_1 k_2} \frac{\pi}{2} \delta \left(k_1 - k_2 \right) .$$

For normalization per unit dk interval then

$$\frac{B_0^2}{k^2} \frac{\pi}{2} = 1$$

or

$$B_0 = k(2/\pi)^{1/2}$$

For use in Eq. (7), however, $\left| R_{ps} \right|^2$ must be normalized per unit energy interval. This is accomplished by multiplying B_0 by

$$\left(\frac{dk}{dE} \right)^{1/2} = \left(\frac{\mu}{\hbar^2 k} \right)^{1/2}$$

so that

$$B_0 \left(\frac{dk}{dE} \right)^{1/2} = \left(\frac{\mu k}{\hbar^2} \frac{2}{\pi} \right)^{1/2} .$$

In order to determine R_{ps} it is now only necessary to subsitute the normalized wave functions into Eq. (6) and integrate. This is a lengthy but straightforward integration, resulting in

$$R_{ps} = \frac{B_1 \; a^2 \left[(2/\pi)\,(\mu k/\hbar^2) \right]^{1/2}}{r_0 \,(k^2 + \gamma^2 \cot^2 \gamma r_0)^{1/2}} \left\{ \frac{2 + 2\,(\beta^2/a^2)\,(1 + ar_0) - r_0^2\,(\gamma^2 - \beta^2)}{(\gamma^2 - \beta^2)^2} \right.$$

$$+ \frac{ar_0 (2 + ar_0) + k^2 r_0^2}{(a^2 + k^2)^2} + \left[- \frac{2 + \left[(\gamma^2 - \beta^2)/a^2 \right] (1 + ar_0)}{(\gamma^2 - \beta^2)^2} \right.$$

$$\left. \left. + \frac{3 + ar_0 + (k^2/a^2)\,(1 + ar_0)}{(a^2 + k^2)^2} \right] \gamma r_0 \cot \gamma r_0 \right\}.$$

APPENDIX B

CORRECTIONS TO THE CROSS SECTION

It is necessary to make several corrections to the cross section computed from the basic formula

$$\sigma = \frac{N_n \, A_{Be}}{N_\gamma \, N_0 \, \rho_{Be} \, \Delta r}$$

These will be described in the following paragraphs.

1. Finite source size. We follow the derivation given by Gibbons et al. (Gi59) .

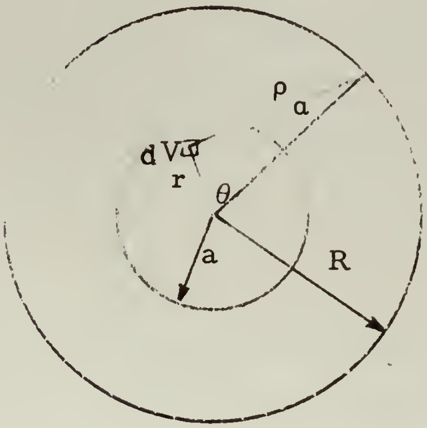

$$\rho^2 = R^2 + r^2 - 2Rr \cos\theta$$

Assuming a homogeneous spherical source of strength Q and radius a, the strength per unit volume is $\frac{3Q}{4\pi a^3}$.

If Nt = number of atoms/cm^2 in the Be shell, then

$$dn = Nt\sigma \frac{R^2}{\rho^2} \frac{3Q}{4\pi a^3} dV$$

gives the number of neutrons per second due to source element dV. The total neutron flux produced is $n_0 f$ where $n_0 = Nt\sigma Q$ is the result if the source were concentrated in a point at the center of the shell, and f is the finite source size correction given by:

$$f = \frac{R^2}{V}\int\frac{dV}{\rho^2} = \frac{3R^2}{4\pi a^3}\iiint_V \frac{r^2 \sin\theta \, dr \, d\theta \, d\phi}{R^2 + r^2 - 2Rr\cos\theta} .$$

This integrates to

$$f = \frac{3R}{2a^3}\left[Ra - \frac{R^2 - a^2}{2} \ln\left(\frac{R+a}{R-a}\right)\right] .$$

Since a << R, the logarithm may be expanded:

$$\ln x = 2\left[\frac{x-1}{x+1} + \frac{1}{3}\left(\frac{x-1}{x+1}\right)^3 + \frac{1}{5}\left(\frac{x-1}{x+1}\right)^5 + \ldots\right] . \quad (x>0)$$

Letting $x = \frac{R+a}{R-a}$; $\frac{x-1}{x+1} = \frac{R}{a}$

$$\ln x = \frac{2a}{R}\left[1 + \frac{1}{3}\left(\frac{a}{R}\right)^2 + \frac{1}{5}\left(\frac{a}{R}\right)^4 + \ldots\right] .$$

Subsituting in the equation for f:

$$f = \frac{3}{2a^2}\left[\frac{2}{3}a^2 + \frac{2}{15}\frac{a^4}{R^2} + \frac{1}{5}\frac{a^6}{R^4} + \ldots\right]$$

$$f \cong 1 + \frac{a^2}{5R^2} .$$

For extreme accuracy this should be multiplied by the average value of sec α, but this correction is negligible when a << R.

2. Attenuation of gamma ray in Be shell.

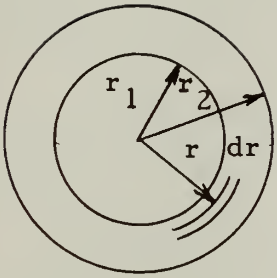

$$\frac{I}{I_0} = \frac{\int_{r_1}^{r_2} e^{-\mu(r-r_1)} dr}{r_2 - r_1}$$

$$= \frac{1}{\mu(r_2-r_1)} \left[\mu(r_2-r_1) - \frac{\mu^2(r_2-r_1)^2}{2} + \ldots \right]$$

$$\frac{I}{I_0} \cong 1 - \frac{\mu(r_2-r_1)}{2}$$

3. Effect of the 2.09-Mev gamma ray.

In the case of the Sb-Be source assembly, the neutron flux measured in the manganous sulfate bath includes not only the neutrons produced by the 1.692-Mev gamma ray, but also those produced by the 2.09-Mev gamma ray. A correction for this effect must be made in computing the cross section at 1.692 Mev. The ratio of the 2.09-Mev gamma ray to the 1.69-Mev gamma ray was measured as 0.148 ± 0.008 by NaI counting. A cross section of 0.4 mb was assumed as a reasonable value at 2.09 Mev. The correction to be applied to the cross section is then

$$0.148 \times 0.4 = 0.06 \text{ mb}.$$

This was divided by the computed cross section to give a percentage correction. Our correction is the same as that applied by Gibbons et al. (Gi59).

4. Neutron escape from $MnSO_4$ bath.

Neutron escape from the $MnSO_4$ bath was significant only in the case of the NBS standard source. This correction was computed by dividing the outer boundary of the bath into zones, computing the neutron flux in each surface zone, and weighting by the solid angle subtended at the center of the bath. The fraction f of neutrons escaping in each zone was computed by the formula

$$f = \frac{\phi}{\phi_0} = 1.5e^{-0.1r}, \qquad \text{(Ge59)}$$

where r is the distance from the source to the edge of the tank in centimeters.

d/r

LEGAL NOTICE